Transportation Research Part B 90 (2016) 172–191

Contents lists available at ScienceDirect

Transportation Research Part B

journal homepage: www.elsevier.com/locate/trb

Enhanced cooperative car-following traffic model with the combination of V2V and V2I communication

Dongyao Jia, Dong Ngoduy*

Institute for Transport Studies, The University of Leeds, Leeds LS2 9JT, United Kingdom

ARTICLE INFO

Article history:
Received 22 December 2015
Revised 24 March 2016
Accepted 25 March 2016
Available online 11 May 2016

Keywords:
Connected vehicle
Cooperative driving
V2V communication
V2I communication
Consensus control
Traffic flow stability

ABSTRACT

Vehicle-to-vehicle (V2V) and vehicle-to-infrastructure (V2I) communication are emerging components of intelligent transport systems (ITS) based on which vehicles can drive in a cooperative way and, hence, significantly improve traffic flow efficiency. However, due to the high vehicle mobility, the unreliable vehicular communications such as packet loss and transmission delay can impair the performance of the cooperative driving system (CDS). In addition, the downstream traffic information collected by roadside sensors in the V2I communication may introduce measurement errors, which also affect the performance of the CDS. The goal of this paper is to bridge the gap between traffic flow modelling and communication approaches in order to build up better cooperative traffic systems. To this end, we aim to develop an enhanced cooperative microscopic (car-following) traffic model considering V2V and V2I communication (or V2X for short), and investigate how vehicular communications affect the vehicle cooperative driving, especially in traffic disturbance scenarios. For these purposes, we design a novel consensus-based vehicle control algorithm for the CDS, in which not only the local traffic flow stability is guaranteed, but also the shock waves are supposed to be smoothed. The IEEE 802.11p, the defacto vehicular networking standard, is selected as the communication protocols, and the roadside sensors are deployed to collect the average speed in the targeted area as the downstream traffic reference. Specifically, the imperfections of vehicular communication as well as the measured information noise are taken into account. Numerical results show the efficiency of the proposed scheme. This paper attempts to theoretically investigate the relationship between vehicular communications and cooperative driving, which is needed for the future deployment of both connected vehicles and infrastructure (i.e. V2X).

1. Introduction

The recent development of information and communication technologies (ICT) facilitates a promising *cooperative driving* which has been considered to significantly improve traffic flow efficiency and traffic safety (van Arem et al., 2006; Kesting et al., 2008; Ngoduy and Jia, 2016; Wang et al., 2014; 2013). Such a cooperative driving system (CDS) can be achieved via the vehicle-to-vehicle (V2V) and vehicle-to-infrastructure (V2I) communication, or V2X for short, which are novel parts of the intelligent transport systems (ITS). To describe the dynamics of traffic flow considering the CDS, we adopt the car-following modelling approach which seeks to describe the movement of individual vehicles at hight level of detail. In general, the

* Corresponding author. Tel.: +44 1133435345.
E-mail address: d.ngoduy@leeds.ac.uk (D. Ngoduy).

http://dx.doi.org/10.1016/j.trb.2016.03.008
0191-2615/

car-following models are usually used to describe the observed human behaviour when driving on road such as acceleration/deceleration, lane changing, etc. (Kesting et al., 2010a; 2008; Laval and Leclercq, 2008; Laval et al., 2014; Saifuzzaman and Zheng, 2014; Saifuzzaman et al., 2015; Treiber et al., 2006; Zheng, 2014; Zheng et al., 2013), but very few has been developed to capture the impact of both V2V and V2I communication, especially how the imperfections of vehicular communication and measured information noise are taken into account in the realistic communication protocols. As an extension of our previous work (Jia and Ngoduy, 2015), which developed a car-following model considering the V2V communication, this paper attempts to theoretically investigate the relationship between both V2V and V2I communication (i.e. V2X) and cooperative driving in a car-following model, which is needed for the future deployment of both connected vehicles and infrastructure. It shall be noted that in this paper we only consider the intelligent traffic flow composed of fully connected and autonomous vehicles.

Basically, in a Cooperative Driving System (CDS), a vehicle obtains neighbouring information via inter-vehicle communication (IVC), and then adopts a suitable control law to achieve a certain objective, such as maintaining a constant inter-vehicle spacing within the same platoon. To this end, four major components in the CDS are supposed to be considered: (1) the vehicle dynamics which inherently characterise vehicle's behaviour stemming from manufacture, e.g., actuator lag; (2) the information to be exchanged among vehicles, e.g., the position and velocity of a vehicle; (3) the communication topology describing the connectivity structure of vehicular networks, such as predecessor-follower, leader-follower, bidirectional, etc.; (4) the control law such as sliding-mode control, consensus control, etc. to be implemented on each vehicle in order to define the car-following rule in the connected traffic flow.

The issues of CDS have been extensively studied in recent years (see Jia et al., 2016 and references there-in). One general design of cooperative adaptive cruise control (CACC) system was proposed in Naus et al. (2010), which adopted the constant time-headway policy in a decentralised control framework, wherein the vehicle only communicates with its directly preceding one. In addition, with the increasing market penetration rate of autonomous car, the issue of autonomous cars and human-driven cars coexisting on the road cannot be neglected. To this end, some recent work has been concerning the effect of the distribution patterns of vehicles equipped with inter-vehicle communications (IVC) on how information propagates (Jin and Recker, 2006; Wang, 2007; Wang et al., 2010), the impact of the penetration of intelligent vehicles on the multi-class traffic flow stability (Ngoduy, 2013a), and how the mixed operation of the different vehicle classes affects the stability of traffic flow (Ngoduy, 2015),

In general, the CDS is based on wireless communication among vehicles (V2V) and between vehicles and the infrastructure (V2I). Basically, the V2V communication helps a vehicle timely collect its neighbours' kinetic information, and based on the obtained traffic information, the vehicle can maintain state convergence to adjacent vehicles in a cooperative way. One typical application is the so-called platoon-based cooperative driving (Fernandes, 2012; Jia et al., 2016; Jia and Ngoduy, 2015; Ngoduy, 2013b). The V2V communication can also provide the information of downstream traffic flow via relay vehicles travelling in the opposite direction to vehicles in the original direction (Kesting et al., 2010b). However, it shall be noted that the *local* traffic information has limited benefit to some traffic applications, such as the route choice and traffic perturbation mitigation. As the wide deployment of networking infrastructures on roadsides, along with the emerging application of cloud computing and big data technologies, a vehicle can also obtain the *front/global* traffic information via V2I communication, which essentially changes the information topology of the CDS (Jin and Wang, 2008). Accordingly, the upstream vehicles can implement suitable countermeasures in advance to any varieties of the downstream traffic flow conditions. Some typical applications include achieving safer and smoother traffic flow (Milanes et al., 2012) and transport energy/emission reductions (Ma and Martensson, 2012).

Although much effort has been undertaken to study the benefit of V2X communication to traffic flow, there are still a few concerns about the practical implementation of such systems. In our view, among a few main challenges are the natural limitations and uncertainties in practical vehicular networking, such as transmission range, packet loss, and probabilistic transmission delay. To this end, our goal is to fill in a gap between traffic flow modelling and communication approaches in order to build a better cooperative traffic system considering such communication problems. Specifically, we consider the issue of traffic shock waves caused by bottleneck or irregular driving behaviour, investigate how to mitigate the negative impact of the speed fluctuation, and meanwhile maintain the local traffic stability with the help of V2X communication. Several studies have been conducted on the shock waves mitigation with the help of vehicular communications. Forster et al. (2014) proposed the so-called "DRIVE" protocol to mitigate shock waves, in which the following vehicles adapt their velocities according to the downstream traffic information propagated over multiple hops. In Jia et al. (2014), to minimise the negative impact of traffic disturbance, the desired acceleration was estimated for the following vehicles based on the front group vehicles' dynamics.

However, regarding the CDS implementation, there still exist some issues not fully addressed before although substantial work has been concerning how to design the CDS under certain communication constraints and uncertainties (Ghasemi et al., 2013; Hao and Barooah, 2012; Jin and Orosz, 2014; Jin and Recker, 2006; Kesting et al., 2010b; Middleton and Braslavsky, 2012; Oncu et al., 2011; Ploeg et al., 2013; Wang et al., 2014; 2013; Wang, 2007).

(i) It is not clear how to design a suitable driving strategy which can integrate the advantage of both V2V and V2I communication.
(ii) Due to the high traffic mobilities, how the unreliable vehicular communication, such as packet loss and transmission delay, impairs the system performance should be addressed.

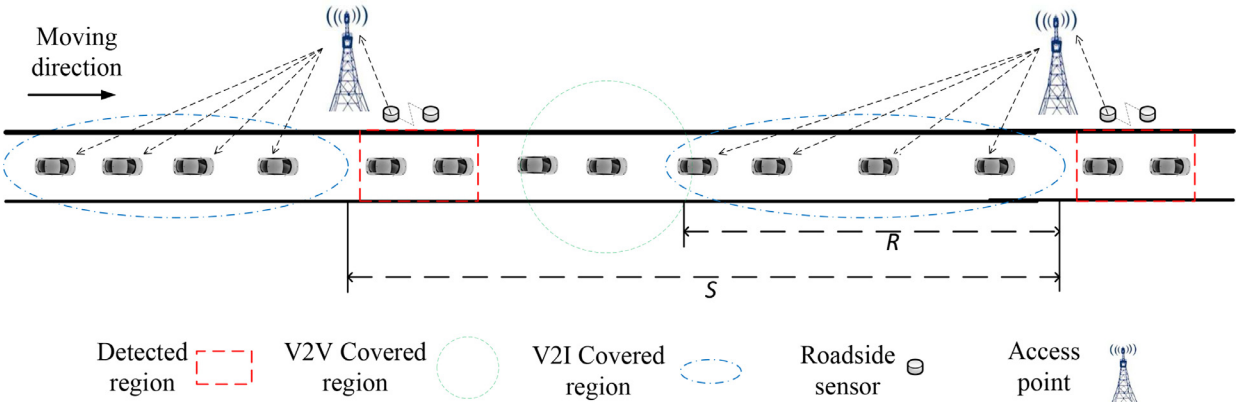

Fig. 1. Cooperative driving with the help of V2X communications.

(iii) It is necessary to explore how the introduced measurement errors (e.g., the downstream traffic information measured by roadside sensors) affect the system performance.

Fig. 1 describes an application scenario of multiple vehicles to drive cooperatively on road with the help of V2X communication, wherein each vehicle periodically broadcasts its kinetic information to the neighbours via V2V communication, and at the same time the downstream traffic dynamics are measured by the roadside sensors and forwarded to the upstream traffic flow via V2I communication.

To identify these issues, in this paper, we aim to build up an enhanced CDS (microscopic) model with the help of both V2V and V2I communication, in which not only the local traffic flow stability is guaranteed, but also the shock waves are supposed to be smoothed. IEEE 802.11p, the defacto vehicular networking standard, is selected as the communication protocols, wherein the imperfections of vehicular communication and measured information noise are taken into account. By definition, the IEEE 802.11p is an approved amendment to the IEEE 802.11 standard to add wireless access in a vehicular communication system. It defines enhancements to 802.11 (the basis of products marketed as Wi-Fi) required to support ITS applications. This IEEE 802.11p supports data exchange between high-speed vehicles and between the vehicles and the roadside infrastructure. More specifically, the *consensus-based* approach is applied into the CDS, which has been regarded as an efficient approach to facilitate the convergence of collective behaviour among multiple agents (Olfati-Saber et al., 2007), and well adapt to the characteristics of the time-varying communication topology of the IVC (Bernardo et al., 2015; Ren, 2007; Wang et al., 2012). In our previous work (Jia and Ngoduy, 2015), we have investigated various (theoretical and numerical) effects of such consensus control law on the dynamics of connected vehicles under V2V communication. To follow our previous approach, in this paper, we will investigate how the consensus control is utilised in the car-following model considering both V2V and V2I communication where the information topology of the CDS essentially changes due to the V2I communication as compared to the CDS under the V2V communication alone. Our main contributions in this paper are threefold.

(i) We design a suitable vehicle driving strategy and propose an *improved consensus-based control* algorithm for the CDS considering V2X communications in a car-following model.
(ii) The effects of V2X communication on system performance, such as transmission delay, transmission coverage, measurement noise etc. are theoretically studied.
(iii) The model is verified by numerical simulations which couple the traffic dynamics and the vehicular communications. More specifically, the system performance is fully evaluated under various traffic scenarios.

The rest of this paper is organised as follows. We first describe the proposed CDS model and formulate the control problem in Section 2. In Section 3, we propose the basic consensus algorithms with only local information by V2V communication, and analyse the system performance under imperfections of vehicular communications. In Section 4, we propose the improved consensus algorithms with both local information and the downstream reference by the combination of V2V and V2I communication, wherein the impacts of the deployment of roadside infrastructure and measurement noise on system performance are taken into account. The simulations are conducted in Section 5 to evaluate the system performance, followed by the conclusion in Section 6.

Notation

For convenience, the notation below will be used for the model development in this paper.

Index	
i, j	vehicle index
t	time instant (s)
Traffic dynamic variables	
p_i	position of vehicle i (m)
v_i	velocity of vehicle i (m/s)
α_i	acceleration of V_L, $\bar{\alpha}$ is the maximum (m/s ^{2})
p_r	position of the downstream reference (m)
v_r	velocity of the downstream reference (m/s)
T	desired time-headway (s)
u_i	control algorithm to minimise state errors
$u_{i,l}$	control algorithm with the only local traffic information
$u_{i,r}$	control algorithm with the only downstream traffic reference
Traffic dynamic parameters	
β_1, β_2, γ_1, γ_2	positive control parameters in control algorithms
θ	weight factor of $u_{i,r}(t)$ over $u_i(t)$
ϵ	velocity measurement error of downstream traffic reference (m/s)
V2X communication parameters	
a_{ij}	communication link from vehicle j to i
τ_j	Beacon dissemination delays from vehicle j to its neighbours (s)
R	V2I transmission range (m)
S	gap between roadside APs (m)
C_r	coverage ratio of V2I communication over the road

2. System modelling

In this section, we first model the traffic dynamics and the IVC, respectively, then demonstrate the specifications and assumptions on the proposed CDS. Finally, we summarise our control objective as well as the corresponding driving strategy.

2.1. Generic car-following model

The dynamics of individual vehicle can be described by microscopic traffic flow models, which illustrate the acceleration of vehicle i in relation to its leading vehicle $(i-1)$. Traditionally, the acceleration of a vehicle is mainly determined by its velocity, the inter-vehicle spacing, and the relative velocity with respect to the leader(s). With the help of the IVC, a vehicle may obtain more information from neighbouring vehicles, which can facilitate the optimal velocity and improve traffic safety and efficiency.

Consider the vehicles i drives cooperatively with its neighbours. At this stage of the paper, we ignore the lane-changing process and only consider the traffic dynamics in a single lane roadway so the neighbouring vehicles refer the the leading vehicles. We assume that in the connected traffic environment the vehicle may obtain local information from its neighbours via V2V communication, as well as the downstream reference from roadside infrastructures via V2I communication. Accordingly, the desired acceleration of vehicle i can be determined in a general form:

$$\frac{dv_i(t)}{dt} \doteq \dot{v}_i(t) = f\left(v_i(t), \Gamma_r(\Delta p_{i,r}(t), \Delta v_{i,r}(t)), \ldots), \Gamma_l(\Delta p_{i,j}(t), \Delta v_{i,j}(t), \ldots)_{j\in\mathcal{G}_l(t)}\right) \tag{1}$$

where $f(.)$ defines a functional form of the car-following model, which will be specified in the ensuing paper taking into account the V2X communication. The reference information $\Delta p_{i,r}(t)$ and $\Delta v_{i,\,r}(t)$ are the position differences and the velocity differences of vehicle i with respect to the downstream front reference. $\Delta p_{i,j}(t)$ and $\Delta v_{i,\,j}(t)$ are the position differences and the velocity differences of vehicle i with respect to its neighbour j, respectively. $\mathcal{G}_l(t)$ denote the time-varying communication topologies formed by vehicle i with its neighbours, while Γ_r and Γ_l describe the corresponding control algorithms, e.g., consensus-based control. This model can be further extended according to the availability of other type of information, e.g., acceleration. We will show in the ensuing paper how the design of V2X communication affects the control algorithms Γ_r and Γ_l. As stated previously, we consider applying the consensus-based control algorithms to regulate the dynamics of vehicle. Specially, the reference information comes not only from the neighbours via V2V communication, but also from the roadside devices with the help of V2I communication.

In this paper, as we only consider the front vehicles the neighbouring vehicles, the forward communication topology is adapted in the envisioned consensus control algorithms, which has been verified to provide a quicker response to the traffic perturbations and a better state convergence of a group of vehicles (Jia and Ngoduy, 2015). The formed vehicular networking topology in V2X communication environment is illustrated in Fig. 2.

2.2. V2V and V2I communication

In the proposed cooperative driving scenario (shown in Fig. 1), each vehicle is supposed to periodically disseminate its current kinematic status (including position, velocity, acceleration, etc.) to its neighbours, namely *beacon message*

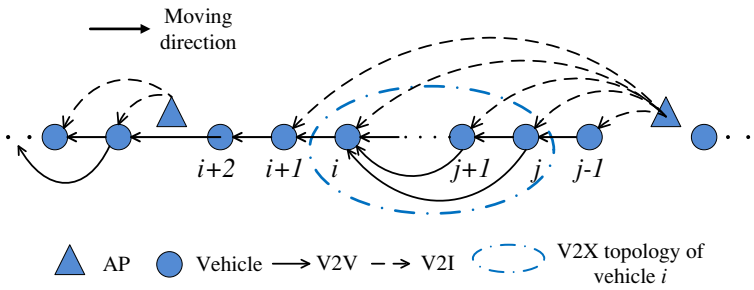

Fig. 2. V2X communication topology for the CDS.

dissemination. Meanwhile, roadside access points (APs) periodically broadcast the traffic information in the targeted area to the upstream vehicles.

In this paper, we assume each vehicle is equipped with on-board sensors to measure its absolute position, speed and acceleration. IEEE Wireless Access in Vehicular Environment (WAVE) suite, the defacto vehicular networking standards, are adopted as the V2V and V2I communication protocols. According to the standard of IEEE 1609.4, all traffic information is broadcasted in the control channel via contention-based carrier sense multiple access with collision avoidance (CSMA/CA) mechanism.

Some specifications and assumptions for the CDS are made as follows.

1. The studied traffic flow is composed of a number of vehicles to drive in the single lane, i.e., lane-changing behaviour is out of discussion in this paper.
2. All vehicles are assumed identical and to drive cooperatively with the constant time headway spacing policy.
3. Roadside APs are uniformly distributed along the road with the gap S, the corresponding fixed transmission range R. Coverage ratio is defined as $C_r = R/S, R \leq S$.
4. The beacon frequency is set $1/\tau$ (typically 10 Hz), and the consensus control is implemented at each end of the control channel interval.
5. The vehicle's acceleration is assumed with an upper bound $\bar{\alpha}$: $\|\dot{v}_i\| = \|\alpha_i\| \leq \bar{\alpha}$.

For vehicular communications, we consider that the communication topology of a CDS can be represented as a directed graph (digraph) $\mathcal{G} = (\mathcal{V}, \mathcal{E}, A)$, where $\mathcal{V} = 1, 2, \ldots, n$ is the set of nodes, $\mathcal{E} \subseteq \mathcal{V} \times \mathcal{V}$ is the set of edges. The set of the neighbours of vehicle i is denoted by $\mathcal{N}_i = \{j \in \mathcal{V} : (j, i) \in \mathcal{E}, j \neq i\}$, and $A = [a_{ij}] \in \mathbb{R}^{n \times n}$ is an adjacency matrix with nonnegative elements which represent the communication link between node i and j. In this paper, we assume $a_{ij} = 1$ in the presence of a communication link from node j to node i, otherwise $a_{ij} = 0$. In addition, we assume no self-loops in the directed graph, i.e., $a_{ii} = 0$ for all $i = 1, \ldots, n$. The degree matrix $D = diag\{d_1, \ldots, d_n\}$ is diagonal matrix, whose diagonal elements are given by $d_i = \sum_{j=1}^{n} a_{ij}$. The Laplacian matrix of the weighted digraph is defined as $L = D - A$, and $\Lambda^+(L)$ denotes the set of nonzero eigenvalues of L.

2.3. Control objectives and driving strategy

The continuous-time dynamics of vehicle i can be represented as follows:

$$\dot{p}_i(t) = v_i(t) \tag{2}$$

$$\dot{v}_i(t) = u_i(t) \tag{3}$$

where $p_i \in R$, $v_i \geq 0$ are the position and velocity of vehicle i, respectively. $u_i \in R$ is the control input, which essentially reflects the acceleration of vehicle i.

For the envisioned CDS, not only the local traffic stability is guaranteed, but also traffic flow fluctuations are supposed to be mitigated. As the constant time-headway spacing policy is adopted in the CDS, the position of vehicle i is supposed to be $p_i = p_0 - i \cdot v_i \cdot T$, where p_0 is the position of the leading vehicle, and T is the desired constant time headway. However, due to the inaccessible information of the leading vehicle in most cases, we define the local stability with the reference of the neighbouring vehicles.

Definition 1 (Local stability)**.** Given the system Eqs. (2) and (3), $\forall j \in \mathcal{N}_i$, if the state of vehicle i satisfies

$$\lim_{t->\infty} |p_j(t) - p_i(t) + (j \cdot v_j - i \cdot v_i) \cdot T| \leq C_p, \lim_{t->\infty} |v_j(t) - v_i(t)| \leq C_v, \tag{4}$$

where C_p and C_v are the constant positive bounded values, then vehicle i is said to reach the local stability.

In Eq. (4), $|p_j(t) - p_i(t) + (j \cdot v_j - i \cdot v_i) \cdot T|$ calculates the position error between the actual gap of vehicle j and i (i.e. $p_j(t) - p_i(t)$), and expected gap (i.e. $(i \cdot v_i - j \cdot v_j) \cdot T$), while $|v_j(t) - v_i(t)|$ calculates the speed errors between vehicle j

and i. That is, the expected gap is proportional to $(j-i)$ under the constant time headway policy, which does not mean the position error bound C_p is proportional to $(j-i)$. In that sense, the relationship between C_p and C_v is not proportional. It shall be noted that the definition of state errors is different from that of the traditional preceding-follower. This is because in the context of V2X communication, the reference information is obtained from not only the preceding vehicle, but also from the further leading ones.

Physically, the above definition indicates that if several vehicles in close proximity can drive at the same speed and maintain the same constant headway among each other, we then say the traffic flow is locally stable, which essentially defines the traffic flow stability from the microscopic perspective.

In addition, we also give an intuitive description of *traffic flow stability*: for the traffic flow with a large number of vehicles, if the further upstream vehicles can simultaneously respond to the leading vehicle's dynamics in case of traffic perturbation, the traffic flow maintains stable. The traffic flow stability will be utilised to evaluate the performance of the proposed driving control algorithms.

To meet the aforementioned objectives, it is critical to design a suitable driving strategy. Normally a vehicle has two typical operational modes: *speed control mode* and *headway control mode*. In case of no front vehicle or enough distance left from the front one, a vehicle can drive at the desired speed which is called speed control model. If the desired speed is greater than that of the preceding vehicle, the gap between the two vehicles will gradually shrink. When the gap decreases to a certain value, namely switching point, the driving controller is supposed to switch from speed control mode to headway control mode, in which the vehicle maintains the desired headway distance with the preceding one.

Clearly, three important issues should be identified for such a driving strategy: speed control, switching point, and headway control. For the speed control, a vehicle is required to follow the predefined desired speed. The switching point can be set as a certain appropriate time-headway, normally larger than the desired time-headway. To maintain a desired headway distance, we propose an improved consensus-based vehicle control algorithm with both the local traffic information and the downstream reference. As illustrated in Fig. 1, we assume that the APs are uniformly distributed along the road, and consider one segment that a vehicle passes through any two adjacent APs. The envisioned control input of vehicle i can be described as:

$$u_i(t) = (1-\theta)u_{i,l}(t) + \theta u_{i,r}(t)\Theta(p_i - S + R) \tag{5}$$

where $u_{i,l}$ is the control algorithm with the local traffic information, $u_{i,r}$ is the control algorithm with the downstream traffic reference, $\theta \in [0, 1]$ is the weight factor to balance the impact of V2V information and V2I information on the system, and $\Theta(a)$ is the Heaviside step function (which is equal to 0 for $a \leq 0$ and equal to 1 otherwise) served as the cutoff for vehicles not obtaining the downstream reference (outside the coverage of the AP).

In the following sections, we first investigate the system performance under the consensus-based control with local information only, then analyze it under the consensus-based control with the additional consideration of the downstream reference.

3. Basic consensus algorithm with local information

3.1. Basic consensus algorithm

To guarantee the local stability of traffic flow, we design the consensus control algorithm for vehicle i with the reference of its neighbouring information, in which the heterogeneous communication delays are taken into account:

$$u_{i,l}(t) = \sum_{j=1}^{n} a_{ij}\{\gamma_1[p_j(t-\tau_j) - p_i(t-\tau_i) + (j\cdot v_j(t-\tau_j) - i\cdot v_i(t-\tau_i))\cdot T] + \gamma_2[v_j(t-\tau_j) - v_i(t-\tau_i)]\} \tag{6}$$

where γ_1 and γ_2 are the positive control parameters. τ_j is the time-varying communication delays from vehicle j to its neighbours (Here we neglect the effect of position difference and assume that all neighbouring vehicles can simultaneously receive the beacon from vehicle j).

Based on the proposed consensus algorithm, we can see the desired acceleration is determined by the state difference (position and velocity) between itself and the neighbours. The first line of Eq. (6) represents the estimated position error between the gap of member i and j at time t with respect to the desired constant time headway spacing of $(j\cdot v_j(t-\tau_j) - i\cdot v_i(t-\tau_i))\cdot T$, while the second line denotes the velocity error between member i and j.

The edges associated with time delay τ_j define a subgraph $\mathcal{G}_j$ with corresponding degree matrix D_j and adjacency matrix A_j, where A_j indicates the communication topology that vehicle j broadcasts information to the neighbours. Clearly, $D = \sum_{j=1}^{n} D_j$ and $A = \sum_{j=1}^{n} A_j$. For the proposed beacon transmission scheme,

$$A_j = \begin{pmatrix} 0 & \cdots & a_{1j} & \cdots & 0 \\ 0 & \cdots & a_{2j} & \cdots & 0 \\ \vdots & \vdots & \vdots & \vdots & \vdots \\ 0 & \cdots & a_{nj} & \cdots & 0 \end{pmatrix}$$

Let $x_i = p_i + i \cdot v_i \cdot T$, then Eq. (6) is transformed to:

$$u_{i,l}(t) = \sum_{j=1}^{n} a_{ij}\{\gamma_1[x_j(t-\tau_j) - x_i(t-\tau_j)] + \gamma_2[v_j(t-\tau_j) - v_i(t-\tau_i)]\} \tag{7}$$

For the traffic flow with nearly constant speed, $\dot{x}_i = \dot{p}_i + i \cdot \dot{v}_i \cdot T \approx \dot{p}_i = v_i$. Then Eqs. (2) and (3) are transformed to:

$$\dot{x}_i(t) = v_i(t) \tag{8}$$

$$\dot{v}_i(t) = u_{i,l}(t) = \sum_{j=1}^{n} a_{ij}\{\gamma_1[x_j(t-\tau_j) - x_i(t-\tau_j)] + \gamma_2[v_j(t-\tau_j) - v_i(t-\tau_i)]\} \tag{9}$$

Let $x \triangleq [x_1, \ldots, x_n]^T, v \triangleq [v_1, \ldots, v_n]^T$, $\chi \triangleq [x^T v^T]^T$, then we can obtain the closed-loop system as follows:

$$\dot{\chi}(t) = \mathcal{A}_0 \chi(t) + \sum_{j=1}^{n} \mathcal{A}_j \chi(t-\tau_j) \tag{10}$$

where

$$\mathcal{A}_0 = \begin{bmatrix} 0_{n\times n} & I_n \\ 0_{n\times n} & 0_{n\times n} \end{bmatrix} \quad \text{and} \quad \mathcal{A}_j = \begin{bmatrix} 0_{n\times n} & 0_{n\times n} \\ \gamma_1(-D_j + A_j) & \gamma_2(-D_j + A_j) \end{bmatrix}$$

By the Leibniz–Newton formula, we have

$$\begin{aligned} \chi(t-\tau_j) &= \chi(t) - \int_{-\tau_j}^{0} \dot{\chi}(t+s)ds \\ &= \chi(t) - \sum_{i=0}^{n} \mathcal{A}_i \int_{-\tau_j}^{0} \chi(t+s-\tau_i)ds \end{aligned} \tag{11}$$

where $\tau_0 \equiv 0$. To substitute Eq. (11) into Eq. (10), we can obtain

$$\dot{\chi}(t) = F\chi(t) - \sum_{j=1}^{n}\sum_{i=0}^{n} \mathcal{A}_j\mathcal{A}_i \int_{-\tau_j}^{0} \chi(t+s-\tau_i)ds \tag{12}$$

where

$$F = \sum_{i=0}^{n} \mathcal{A}_i = \begin{bmatrix} 0_{n\times n} & I_n \\ -\gamma_1 L & -\gamma_2 L \end{bmatrix}$$

3.2. Local stability analysis

For the sake of simplicity, we assume that the heterogeneous delays τ_j are set to a unique constant value τ. Accordingly, Eq. (12) can be rewritten as:

$$\dot{\chi}(t) = F\chi(t) - \mathcal{B}\mathcal{A}_0 \int_{-\tau}^{0} \chi(t+s)ds - \mathcal{B}^2 \int_{-\tau}^{0} \chi(t+s-\tau)ds \tag{13}$$

where

$$\mathcal{B} = \begin{bmatrix} 0_{n\times n} & 0_{n\times n} \\ -\gamma_1 L & -\gamma_2 L \end{bmatrix}$$

According to Ren and Beard (2005), if $\mathcal{G}$ has a directed spanning tree, L has a simple zero eigenvalue and all other eigenvalues are on the open right half-plane, then we can choose an orthonormal basis of $\mathbb{R}^N$ matrix with the form $W = [(1/\sqrt{n})\mathbf{1}_n, w_1, \ldots, w_{n-1}] = [(1/\sqrt{n})\mathbf{1}_n, W_1]$, wherein $w_i \in \mathbb{R}^{n\times 1}$ and $W_1 \in \mathbb{R}^{n\times(n-1)}$, to transform L into:

$$W^T L W = \begin{bmatrix} 0 & 0_{n-1}^T \\ 0_{n-1} & \widetilde{L} \end{bmatrix}$$

where all the eigenvalues of $\widetilde{L}$ are on the open right half-plane.

Then we have $W_1^T\mathbf{1} = 0$, $W_1^T W_1 = I_{n-1}$, and $W_1 W_1^T = I_n - 1/n\mathbf{1}\mathbf{1}^T$.

Let $\widetilde{x} = W^T x$, $\widetilde{v} = W^T v$ and $\widetilde{\chi} = [\widetilde{x}^T \widetilde{v}^T]^T$, then Eq. (13) can be transformed into:

$$\dot{\widetilde{\chi}}(t) = \widetilde{F}\widetilde{\chi}(t) - \mathcal{B}_1\mathcal{A}_0 \int_{-\tau}^{0} \widetilde{\chi}(t+s)ds - \mathcal{B}_1^2 \int_{-\tau}^{0} \widetilde{\chi}(t+s-\tau)ds \tag{14}$$

where

$$\widetilde{F} = \begin{bmatrix} 0_{n\times n} & I_n \\ -\gamma_1 W^T L W & -\gamma_2 W^T L W \end{bmatrix} \quad \text{and} \quad \mathcal{B}_1 = \begin{bmatrix} 0_{n\times n} & 0_{n\times n} \\ -\gamma_1 W^T L W & -\gamma_2 W^T L W \end{bmatrix}$$

Let $\widetilde{x}_0$ and $\widetilde{v}_0$ denote the first row of $\widetilde{x}$ and $\widetilde{v}$, respectively. Let $\widetilde{x}_{n-1}$ and $\widetilde{v}_{n-1}$ denote the last $n-1$ rows of $\widetilde{x}$ and $\widetilde{v}$, respectively. Then Eq. (14) can be decoupled into the following two equations:

$$\dot{\widetilde{\chi}}_0(t) = \begin{bmatrix} 0 & 1 \\ 0 & 0 \end{bmatrix} \widetilde{\chi}_0(t) \tag{15a}$$

$$\dot{\widetilde{\chi}}_{n-1}(t) = \widetilde{F}_{n-1}\widetilde{\chi}_{n-1}(t) - \widetilde{\mathcal{B}}_1\widetilde{\mathcal{A}}_0 \int_{-\tau}^{0} \widetilde{\chi}_{n-1}(t+s)ds - \widetilde{\mathcal{B}}_1^2 \int_{-\tau}^{0} \widetilde{\chi}_{n-1}(t+s-\tau_i)ds \tag{15b}$$

where $\widetilde{\chi}_0 = [\widetilde{x}_0^T, \widetilde{v}_0^T]^T$, $\widetilde{\chi}_{n-1} = [\widetilde{x}_{n-1}^T, \widetilde{v}_{n-1}^T]^T$,

$$\widetilde{F}_{n-1} = \begin{bmatrix} 0_{(n-1)\times(n-1)} & I_{n-1} \\ -\gamma_1\widetilde{L} & -\gamma_2\widetilde{L} \end{bmatrix}, \quad \widetilde{\mathcal{B}}_1 = \begin{bmatrix} 0_{(n-1)\times(n-1)} & 0_{(n-1)\times(n-1)} \\ -\gamma_1\widetilde{L} & -\gamma_2\widetilde{L} \end{bmatrix}$$

and

$$\widetilde{\mathcal{A}}_0 = \begin{bmatrix} 0_{(n-1)\times(n-1)} & I_{n-1} \\ 0_{(n-1)\times(n-1)} & 0_{(n-1)\times(n-1)} \end{bmatrix}$$

Thus we have the following Lemmas.

Lemma 1. *The matrix $\widetilde{F}_{n-1}$ is Hurwitz stable if*

$$\frac{\gamma_2}{\sqrt{\gamma_1}} > \max_{\theta_i \in \sigma(\widetilde{L})} \frac{|Im(\theta_i)|}{\sqrt{|Re(\theta_i)| \cdot |\theta_i|}} \tag{16}$$

Proof. See the proof in Appendix A of this paper. □

Before exploring the convergence of proposed local consensus-based algorithms, we first introduce the Lyapunov–Razumikhin Theorem. Let $C([-r,0],\mathbb{R}^n)$ be a Banach space of continuous functions defined on an interval $[-r,0]$ and taking values in $\mathbb{R}^n$ with a norm $\|\phi\|_c = \max_{\theta\in[-r,0]}\|\phi(\theta)\|$. Consider the following time delayed system:

$$\begin{aligned} &\dot{x} = f(t, x_t), \quad t > 0, \\ &x(\theta) = \phi(\theta), \quad \theta \in [-r, 0] \end{aligned} \tag{17}$$

where $x_t(\theta) = x(t+\theta), \forall\theta \in [-r,0]$, $f : \mathbb{R}\times C([-r,0],\mathbb{R}^n) \to \mathbb{R}$ is a continuous function and $f(t,0) = 0, \forall t \in \mathbb{R}$. Then we hold:

Lemma 2 (Lyapunov–Razumikhin Theorem, Hale and Lunel, 1993)**.** *Let ϕ_1, ϕ_2 and ϕ_3 be continuous, nonnegative, nondecreasing functions with $\phi_1(s) > 0$, $\phi_2(s) > 0$ and $\phi_3(s) > 0$ for $s > 0$ and $\phi_1(0) = \phi_2(0) = 0$. If there is a continuous function $V(t, x)$ such that*

$$\phi_1(\|x\|) \le V(t,x) \le \phi_2(\|x\|), \quad t \in \mathbb{R}, x \in \mathbb{R}^n. \tag{18}$$

In addition, there exists a continuous nondecreasing function $\phi(s)$ with $\phi(s) > s$, $s > 0$ such that the derivative of V along the solution $x(t)$ of Eq. (17) satisfies

$$\begin{aligned} &\dot{V}(t,x) \le -\phi_3(\|x\|) \\ &if\, V(t+\theta, x(t+\theta)) < \phi(V(t, x(t))), \quad \theta \in [-r, 0]; \end{aligned} \tag{19}$$

then the solution $x = 0$ is uniformly asymptotically stable.

Thus we have the following theorems.

Theorem 1. *If there exists a spanning tree in the topology graph $\mathcal{G}$, and the control parameters γ_1 and γ_2 satisfy Eq. (16), then there exist a constant $\tau_0 > 0$, such that when $0 \le \tau_j \le \tau_0$ $(j = 1,\ldots, N)$, the vehicle under the proposed consensus control Eq. (6) can achieve the local stability as defined in Eq. (4).*

Proof. See the proof in Appendix B of this paper. □

According to Theorem 1, the proposed consensus algorithm can guarantee the local stability if the transmission delay is less than certain value. In addition, in case of packet loss, the algorithm uses the last available information, which means transmission delay actually jumps, to a large value, then returns to a smaller value when the next valid message is received. Therefore, Theorem 1 holds as well in case of packet loss. To follow the same approach, we can further get the similar result to Theorem 1 in case of the heterogeneous time delay of beacon dissemination. The proofs are omitted here for the sake of brevity.

4. Improved consensus algorithm with the downstream reference

4.1. Improved consensus-based control algorithm

As illustrated in Fig. 1, the roadside sensors timely measure the traffic dynamics within the targeted area, and deliver them to the nearest access point (AP). Thus a vehicle can obtain this downstream traffic information via the periodical broadcast of the AP, and adapt a suitable control strategy to smooth the traffic perturbation. Intuitively, the envisioned control algorithm is to let the upstream vehicles adapt to the downstream traffic state well in advance, i.e., the upstream vehicles are supposed to drive at the same speed and maintain the same constant headway among each other to that of downstream vehicles in the targeted area (with bounded errors), which can be mathematically presented by:

$$\lim_{t->\infty} |p_i(t) + i \cdot v_r \cdot T - p_r(t)| \le C'_p, \lim_{t->\infty} |v_r(t) - v_i(t)| \le C'_v, \tag{20}$$

where C'_p and C'_v is the constant bounded values, v_r is the velocity of the downstream reference equivalent to the mean velocity in the targeted area which can be measured by the roadside sensors, $p_r(t) = \int_0^t v_r ds$ is the virtual position of the downstream reference calculated by the integration of v_r, $v_r \cdot T$ is the expected constant time headway spacing referred to the downstream traffic state. Therefore, the proposed $u_{i,r}$ considering communication delay of V2X is represented as

$$u_{i,r}(t) = \beta_1 \sum_{j=1}^{n} a_{ij}[p_j(t-\tau_j) - p_i(t-\tau_i) + (j-i) \cdot v_r(t-\tau_r) \cdot T] + \beta_2[v_r(t-\tau_r) - v_i(t-\tau_i)] \tag{21}$$

where β_1 and β_2 are the positive control parameters.

In addition, the practically introduced measurement error of the downstream reference by the roadside sensors is considered in the proposed control algorithms. Let $\hat{v}_r(t) = v_r(t) + \epsilon(t)$, where $\epsilon(t)$ is independent measurement error bounded noise which satisfies:

$$\|\epsilon(t)\| \le \bar{\epsilon}, \quad \left\| \int_0^t \epsilon(s) ds \right\| \le \varrho_1, \quad \left\| \int_0^t \int_0^s \epsilon(r) dr ds \right\| \le \varrho_2$$

where ϱ_1, ϱ_2 are some positive constants.

Thus $u_{i,r}$ is given by:

$$\begin{aligned} u_{i,r}(t) &= \beta_1 \sum_{j=1}^{n} a_{ij}[p_j(t-\tau_j) - p_i(t-\tau_i) + (j-i) \cdot \hat{v}_r(t-\tau_r) \cdot T] + \beta_2[\hat{v}_r(t-\tau_r) - v_i(t-\tau_i)] \\ &= \beta_1 \sum_{j=1}^{n} a_{ij}[p_j(t-\tau_j) - p_i(t-\tau_i) + (j-i) \cdot v_r(t-\tau_r) \cdot T] + \beta_2[v_r(t-\tau_r) - v_i(t-\tau_i)] \\ &\quad + \epsilon(t-\tau_r)[\beta_1 \sum_{j=1}^{n} a_{ij}(j-i)T + \beta_2] \end{aligned} \tag{22}$$

For convenience, we define $\delta_i(t-\tau_r) = \epsilon(t-\tau_r)[\beta_1 \sum_{j=1}^{n} a_{ij}(j-i)T + \beta_2]$. Furthermore, if the number of neighbouring vehicle is N for vehicle i, we can calculate the upper bound of δ_i as $\bar{\delta} = \bar{\epsilon}(\frac{N(N+1)}{2}\beta_1 T + \beta_2)$.

Accordingly, combined with Eq. (5), we can obtain the improved consensus-based control algorithms as follows:

$$\begin{aligned} u_i(t) &= (1-\theta) \cdot \sum_{j=1}^{n} a_{ij}\{\gamma_1[p_j(t-\tau_j) - p_i(t-\tau_i) + (j \cdot v_j(t-\tau_j) - i \cdot v_i(t-\tau_i)) \cdot T] + \gamma_2[v_j(t-\tau_j) - v_i(t-\tau_i)]\} \\ &\quad + \theta \cdot \beta_1 \sum_{j=1}^{n} a_{ij}[p_j(t-\tau_j) - p_i(t-\tau_i) + (j-i) \cdot v_r(t-\tau_r) \cdot T] + \beta_2[v_r(t-\tau_r) - v_i(t-\tau_i)] \\ &\quad + \theta \cdot \epsilon(t-\tau_r)[\beta_1 \sum_{j=1}^{n} a_{ij}(j-i)T + \beta_2] \end{aligned} \tag{23}$$

It shall be noted that we do not consider the impact of V2V communication noise in the control algorithm, as all possible signal noises can finally lead to packet loss and transmission delay in the communication, which has been addressed in our previous work (Jia and Ngoduy, 2015). In addition, the V2I transmission power are normally much larger than that of V2V, therefore we disregard the impact of V2V noises on the V2I communication.

4.2. System performance

This section analyzes the local stability under the proposed improved consensus algorithm Eq. (23). We first consider CDS under control algorithm with only downstream reference. Let $x_i = p_i + i \cdot v_r \cdot T$, $\bar{x}_i = x_i - p_r(t)$, $\bar{v}_i = v_i - v_r$, $\bar{x} \triangleq [\bar{x}_1, \ldots, \bar{x}_n]^T$,

$\bar{v} \triangleq [\bar{v}_1, \ldots, \bar{v}_n]^T$, $\bar{\chi} \triangleq [\bar{x}^T \bar{v}^T]^T$, and substitute Eq. (22) into Eqs. (2) and (3), we can derive the closed-loop dynamics of vehicles as follows:

$$\dot{\bar{\chi}}(t) = \mathcal{A}_0 \bar{\chi}(t) + \sum_{j=1}^{n} \mathcal{A}_j \bar{\chi}(t-\tau_j) + \Delta \tag{24}$$

where

$$\mathcal{A}_0 = \begin{bmatrix} 0_{n\times n} & I_n \\ 0_{n\times n} & 0_{n\times n} \end{bmatrix}, \quad \mathcal{A}_j = \begin{bmatrix} 0_{n\times n} & 0_{n\times n} \\ \beta_1(-D_j + A_j) & -\beta_2 I_{n\times n} \end{bmatrix} \quad \text{and} \quad \Delta = \begin{bmatrix} 0_{n\times 1} \\ \delta_{n\times 1}(t) \end{bmatrix}$$

Accordingly, the system can be decoupled into two parts: the neighbouring consensus system and the downstream traffic state error system.

To follow the Leibniz–Newton formula, we have $\bar{\chi}(t-\tau_j) = \bar{\chi}(t) - \int_{-\tau_j}^{0} \dot{\bar{\chi}}(t+s)ds = \bar{\chi}(t) - \sum_{i=0}^{n} \mathcal{A}_i \int_{-\tau_j}^{0} \bar{\chi}(t+s-\tau_i)ds - \int_{-\tau_j}^{0} \Delta(t+s)ds$, where $\tau_0 \equiv 0$. To substitute this equation into Eq. (24), we can obtain

$$\dot{\bar{\chi}}(t) = F\bar{\chi}(t) - \sum_{j=1}^{n}\sum_{i=0}^{n} \mathcal{A}_j\mathcal{A}_i \int_{-\tau_j}^{0} \bar{\chi}(t+s-\tau_i)ds - \sum_{j=1}^{n} \mathcal{A}_j \int_{-\tau_j}^{0} \Delta(t+s)ds + \Delta \tag{25}$$

where

$$F = \sum_{i=0}^{n} \mathcal{A}_i = \begin{bmatrix} 0_{n\times n} & I_n \\ -\beta_1 L & -\beta_2 I_n \end{bmatrix}$$

Similarly, we only consider the heterogeneous delays τ_j being set to a unique constant value τ. Accordingly, Eq. (25) can be transformed to:

$$\dot{\chi}(t) = F\chi(t) - \mathcal{B}\mathcal{A}_0 \int_{-\tau}^{0} \chi(t+s)ds - \mathcal{B}^2 \int_{-\tau}^{0} \chi(t+s-\tau)ds + \Delta \tag{26}$$

where

$$\mathcal{B} = \begin{bmatrix} 0_{n\times n} & 0_{n\times n} \\ -\beta_1 L & -\beta_2 I_n \end{bmatrix}$$

Let $\tilde{x} = W^T\bar{x}$, $\tilde{v} = W^T\bar{v}$, $\tilde{\Delta} = W^T\Delta$, and $\tilde{\chi} = [\tilde{x}^T\tilde{v}^T]^T$, then we adopt the same method in Section 3 to decouple Eq. (26) into the following two equations:

$$\dot{\tilde{\chi}}_0(t) = \begin{bmatrix} 0 & 1 \\ 0 & 0 \end{bmatrix} \tilde{\chi}_0(t) + \tilde{\Delta}_0 \tag{27a}$$

and

$$\dot{\tilde{\chi}}_{n-1}(t) = \tilde{F}_{n-1}\tilde{\chi}_{n-1}(t) - \tilde{\mathcal{B}}_1\tilde{\mathcal{A}}_0 \int_{-\tau}^{0} \tilde{\chi}_{n-1}(t+s)ds - \tilde{\mathcal{B}}_1^2 \int_{-\tau}^{0} \tilde{\chi}_{n-1}(t+s-\tau_i)ds + \tilde{\Delta}_{n-1} \tag{27b}$$

where $\tilde{\chi}_0 = [\tilde{x}_0^T, \tilde{v}_0^T]^T$, $\tilde{\chi}_{n-1} = [\tilde{x}_{n-1}^T, \tilde{v}_{n-1}^T]^T$, $\tilde{\Delta}_0 = [0_{0\times 1}^T, \delta_{0\times 1}(t)^T]^T$, $\tilde{\Delta}_{n-1} = [0_{(n-1)\times 1}^T, \delta_{(n-1)\times 1}^T(t)]^T$,

$$\tilde{F}_{n-1} = \begin{bmatrix} 0_{(n-1)\times(n-1)} & I_{(n-1)\times(n-1)} \\ -\beta_1 L & -\beta_2 I_{n-1} \end{bmatrix}, \quad \tilde{\mathcal{B}}_1 = \begin{bmatrix} 0_{(n-1)\times(n-1)} & 0_{(n-1)\times(n-1)} \\ -\beta_1 L & -\beta_2 I_{n-1} \end{bmatrix}$$

and

$$\tilde{\mathcal{A}}_0 = \begin{bmatrix} 0_{(n-1)\times(n-1)} & I_{n-1} \\ 0_{(n-1)\times(n-1)} & 0_{(n-1)\times(n-1)} \end{bmatrix}$$

Thus we can have the following theorem.

Theorem 2. *If there exists a spanning tree in the topology graph $\mathcal{G}$, under the proposed consensus algorithms (22), and the control parameters β_1 and β_2 satisfy*

$$\begin{bmatrix} \beta_1^2(L+L^T) - \beta_2 I & \beta_1\beta_2(L^T+I) - (\beta_1+\beta_2)I \\ \beta_1\beta_2(L+I) - (\beta_1+\beta_2)I & (2\beta_2^2 - 2\beta_1 - \beta_2)I \end{bmatrix} > 0 \tag{28}$$

then there exist a sufficient small constant $\tau_0 > 0$, such that when $0 \le \tau_j \le \tau_0$ (j = 1,..., N), the state error between the following vehicle and the downstream reference is uniformly ultimately bounded by:

$$\lim_{t\to\infty} \|\bar{\chi}_k\| \le C_0 \tag{29}$$

for some constant C_0 depending on $\bar{\alpha}$, traffic perturbation magnitude, and the measurement noise of the downstream reference.

Table 1
Communication system model setting.

Parameter	Value	Parameter	Value
Communication protocol	802.11p	Channel data rate	6 Mbps
Beacon frequency $1/\tau$	10 Hz	Beacon size	200 bytes
AP's beacon frequency	0.5–10 Hz	AP's coverage	500–2000 m
Sensing coverage	300 m	Vehicle's coverage	200 m
Sensing velocity error ρ_v	0.5, 1, 2	Neighbouring vehicle	1–5

Table 2
Vehicle dynamic parameters.

Parameter	Value	Parameter	Value
Desired time-headway	1 s	Switching point	2 s
Maximum acceleration	3 m/s^2	Maximum deceleration	6 m/s^2
Maximum velocity	41 m/s	Stable speed	25 m/s
Standstill distance	5 m	Vehicle length	5 m
Control parameters:	$\beta_1 = \gamma_1 = 0.2$,	$\beta_2 = \gamma_2 = 0.5$	

Proof. See our proof in Appendix C. □

Furthermore, combining with the result of Theorems 1 and 2, as well as the additivity of the system Eqs. (2) and (3), we can derive that under the improved consensus control algorithm Eq. (23), the state errors between the vehicles are uniformly ultimately bounded, i.e., the local stability defined by Eq. (4) holds. This conclusion could be utilised as a criterion for the safety driving design, that is, to guarantee the collision avoidance between vehicles, the desired inter-vehicle spacing shall be larger than the maximum position errors. In addition, we note that in the proposed consensus control algorithm, the identical factor is set to the reference information of each neighbouring vehicle. To improve the safe driving, the weighted factors could be designed in the control algorithm, e.g., more weight assigned to the ones closer to the considered vehicle.

As a result, a vehicle may adopt two different driving strategies in practice: the basic consensus algorithm with the local traffic information and the improved consensus algorithm with the additional consideration of the downstream traffic reference, which can lead to the drastic changes of the vehicle dynamics (sharp deceleration or acceleration) when switching between the two types of control algorithms. To mitigate this negative impact, θ is supposed to be carefully designed as a continuous function $\theta = f(p_i)$. However, at this proof of concept stage, we simply assume a constant $\theta = 0.5$ for the proposed improved consensus-based control algorithm.

5. Simulations

In this section, we first explain the experiment settings, then conduct a few simulation experiments to evaluate the performance of the proposed consensus-based driving strategies with the help of V2X communications.

5.1. Simulation settings

PLEXE (Segata et al., 2014) simulator is used in this paper, an open source inter-vehicular communication simulation framework which combines OMNeT++ for event-driven network simulation and SUMO for generation of traffic environment and vehicle movement. The system parameters for both communication model and consensus-based control algorithms are specified in Tables 1 and 2, respectively. It shall be noted that to model more realistic vehicle dynamics, the actuator lag (i.e., the delay between the acceleration command and its actual realisation in the vehicle due to inertial and mechanical limits) is considered and implemented in PLEXE. In addition, to eliminate the impact of practical heterogeneous delay in V2V communication, we let $p_i(t-\tau_i) = p_i(t-\tau) + v_i(t-\tau_i)(\tau-\tau_i)$ and $v_i(t-\tau_i) \approx v_i(t-\tau))$ in Eq. (6), and thus the heterogeneous delays τ_j are changed to a unique constant value τ.

Three typical traffic scenarios are considered for the system evaluation: (1) The stable traffic flow wherein all vehicles drive at the same constant speed 25 m/s, (2) The single large perturbation where the leading vehicle first experiences a deceleration phase with 4 m^2/s from 25 m/s to 5 m/s, then maintains the lower speed of 5 m/s for time of 160 s, and finally accelerates with 2 m^2/s from 5 m/s to 25 m/s, and (3)the continuous small perturbations where the leading vehicle experience a sinusoidal disturbance defined by:

$$\delta(t) = A\sin(0.2\pi t), \quad A = 5\,\text{m/s} \tag{30}$$

We consider two possible traffic flow distributions in view of connection topology at the initial stage: (**I**) the *fully connected traffic flow* in which all inter-vehicle spacings are less than the vehicle's coverage, i.e., each vehicle can obtain the information of the preceding one via V2V communication, and (**II**) the *partially connected traffic flow* wherein some inter-vehicle spacings are larger than the vehicle's coverage, which means some vehicles' information is unavailable to the following ones. In the following simulations, we specify the fully connected traffic flow **I** consisting of 20 vehicles initially

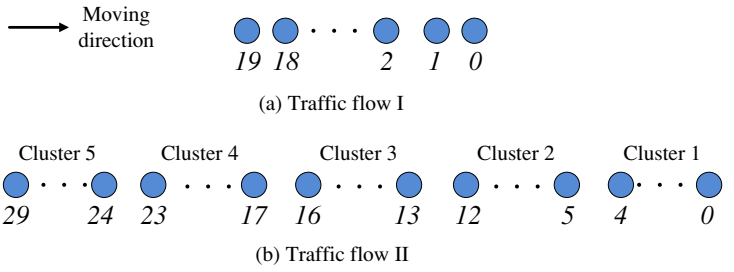

Fig. 3. Testing traffic flow.

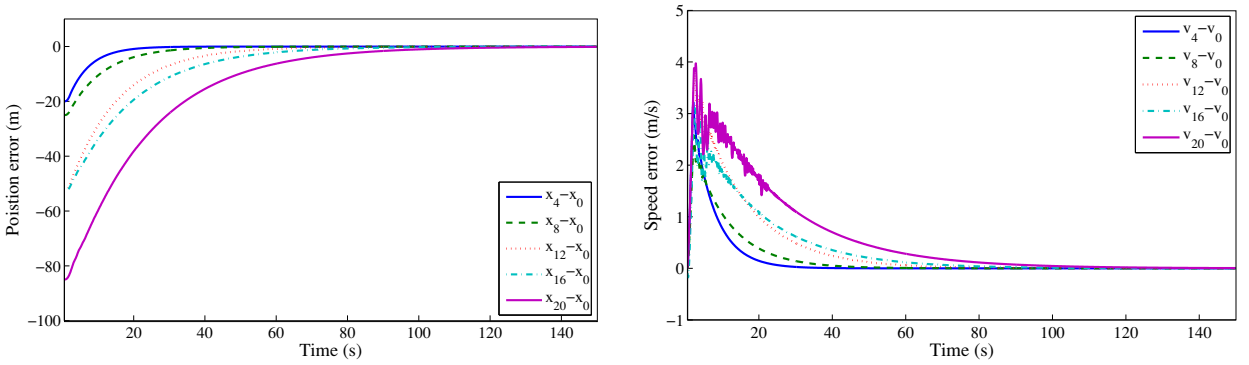

(a) Position error (b) Speed error

Fig. 4. State error of vehicles in traffic flow **I** at the desired constant speed scenario.

randomly distributed with the mean inter-vehicle distance of 40m, while the partially connected traffic flow **II** initially being composed of 30 vehicles randomly formed into 5 clusters (5, 8, 4, 7, 6) with the mean distance of 300m among clusters. The testing traffic flow is illustrated in Fig. 3. It is worth mentioning that in the simulation we label the leading vehicle as 0.

5.2. Basic traffic control with local information

In this section, we evaluate the vehicle driving performance by the control algorithm Eq. (6) with the local information in different traffic scenarios.

We first consider the stable traffic scenario wherein all vehicles drive at the desired constant-speed. The desired inter-vehicle spacing in this condition is calculated by speed · timeheadway+standstill+vehiclelength=35 m, and the neighbouring number (i.e. the number of leading vehicles will can provide information to the considered vehicle) is set to 3. Fig. 4 plots the state errors of each vehicle with respect to its neighbours in traffic flow **I**. It is observed that the state (both position and velocity) errors can converge to zero as time increases, which means the vehicle local stability can be guaranteed under the proposed basic consensus control algorithm. As a result, the initially randomly distributed traffic flow **I** finally forms into a long platoon with the same constant time-headway spacing.

Moreover, by comparing the system performance with different setting of neighbouring number, as shown in Fig. 5, we can observe that the more leading vehicles which can provide information to the considered vehicle, the less state error variation appeared at the initial phase. However, this improvement is trivial when the neighbouring number exceeds certain value (e.g., 3). This is consistent with findings in Ngoduy (2013b) and Ngoduy and Wilson (2014).

Likewise, we evaluate the partially connected traffic flow **II** wherein some initial inter-vehicle spacing are larger than the vehicle's coverage, as shown in Fig. 6. We can observe that under the control algorithm Eq. (6), the initial 5 clusters with uneven inter-vehicle spacing traffic flow finally forms into a series of stable regular platoons with different platoon size, in which inter-vehicle spacing is 35m and each vehicle's speed is 25 m/s. Consequently, it is clear that in the stable traffic condition, the proposed local consensus control may form traffic flow **I** into a long platoon with the same constant time-headway spacing, whilst distributing the traffic flow **II** into a series of independent platoons with no interference among each other.

Next, we evaluate the system performance under two typical perturbation scenarios: the single large perturbation (to mimic traffic emergency like collision avoidance) and the continuous small perturbations of the leader speed (to mimic common traffic disturbance caused by abnormal driving behaviour).

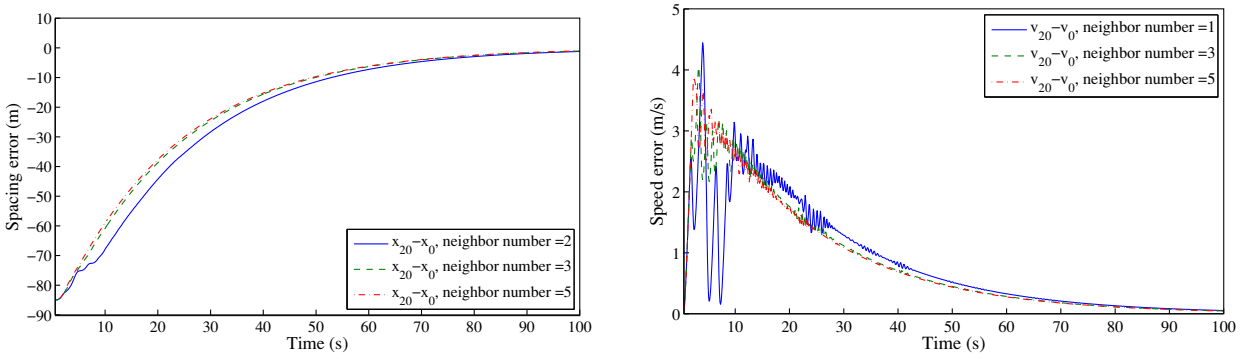

(a) Position error (b) Speed error

Fig. 5. The impact of neighbouring number for traffic flow **I** at the desired constant speed scenario .

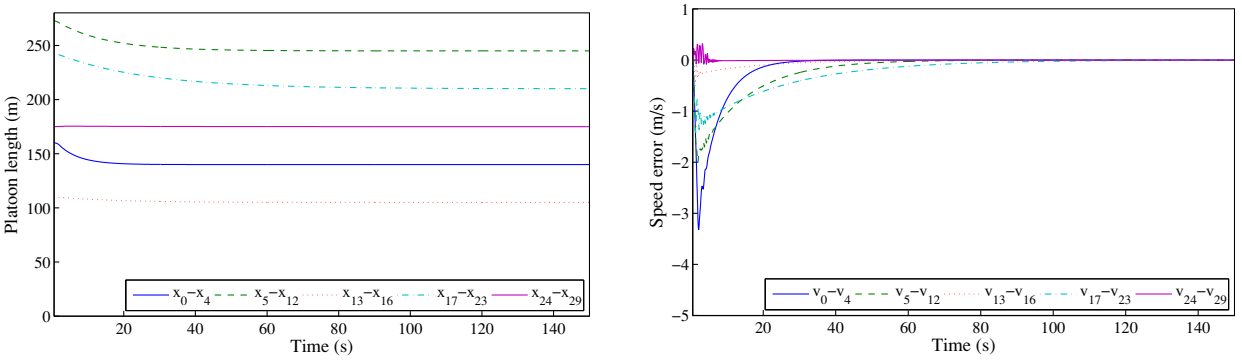

(a) Platoon length (b) Speed error

Fig. 6. Traffic flow **II** at the desired constant speed scenario.

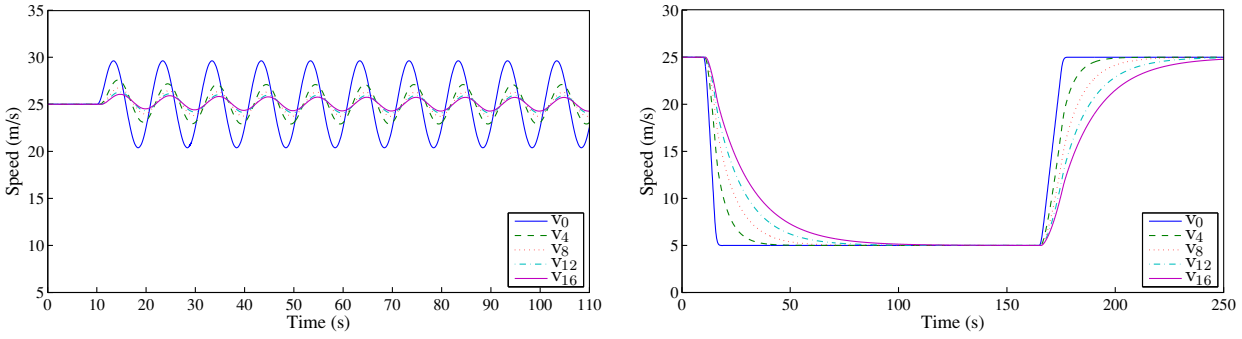

(a) Continuous small traffic perturbations (b) Single large perturbation

Fig. 7. Speed of traffic flow **I** with local information in different perturbations scenarios.

The simulation results for the traffic flow **I** are given in Figs. 7 and 8, respectively. We can see that due to the full communication connectivity, almost all vehicles started to decelerate/accelerate simultaneously. The traffic perturbations are significantly mitigated along the upstream direction, which displays the effectiveness of the constant time-headway policy, rather than the constant spacing-headway (Jia and Ngoduy, 2015), adopted in the proposed control algorithm. In addition, the bounded errors of inter-vehicle spacing between the leading vehicle and the follower are gradually attenuated along the upstream in both scenarios, which validates the (guaranteed) local stability under the proposed consensus algorithms.

By contrast, we can observe that for traffic flow **II**, the vehicles in different clusters started to decelerate/accelerate asynchronously in both perturbation scenarios due to the disconnection between clusters, as shown in Fig. 9. As a result, the perturbation propagation can be blocked from the first cluster to the following ones in case of continuous small traffic perturbations (see in Fig. 9(a) the speed of the first vehicle in the second cluster v_5 was not affected by the perturbation),

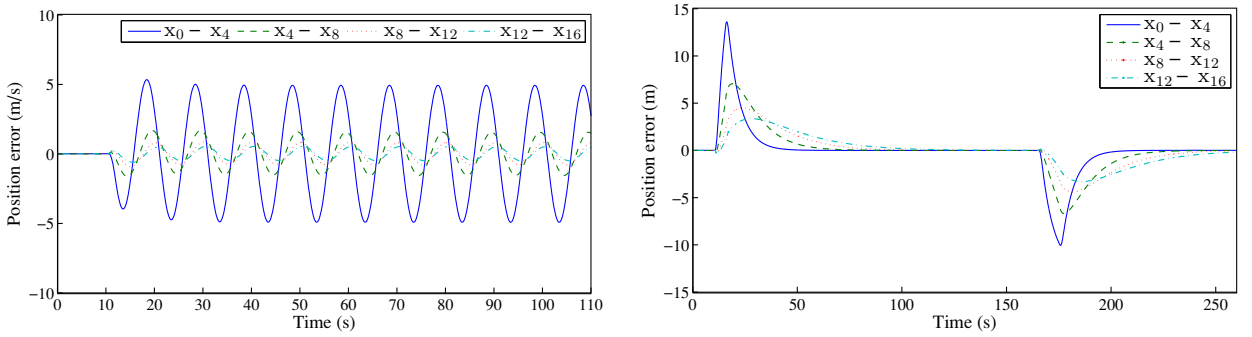

(a) Continuous small traffic perturbations (b) Single large perturbation

Fig. 8. Position error of traffic flow **I** with local information in different perturbations scenarios.

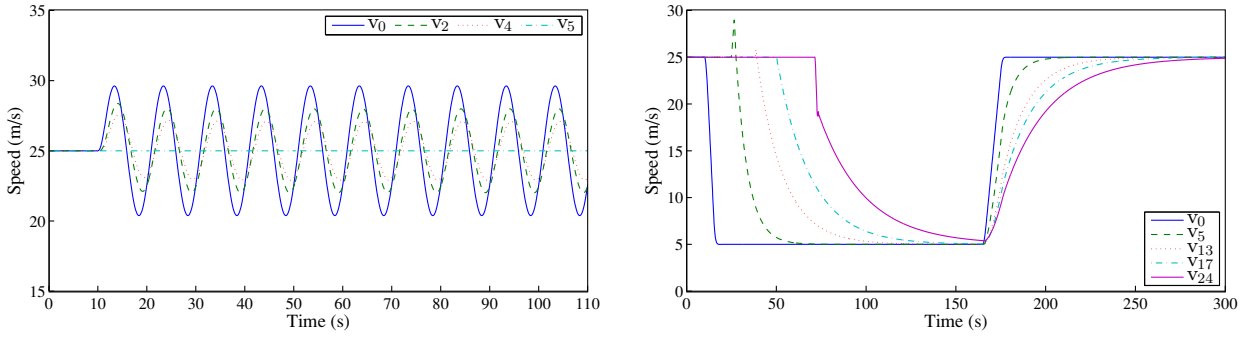

(a) Continuous small traffic perturbations (b) Single large perturbation

Fig. 9. Speed of traffic flow **II** with local information in different perturbations scenarios.

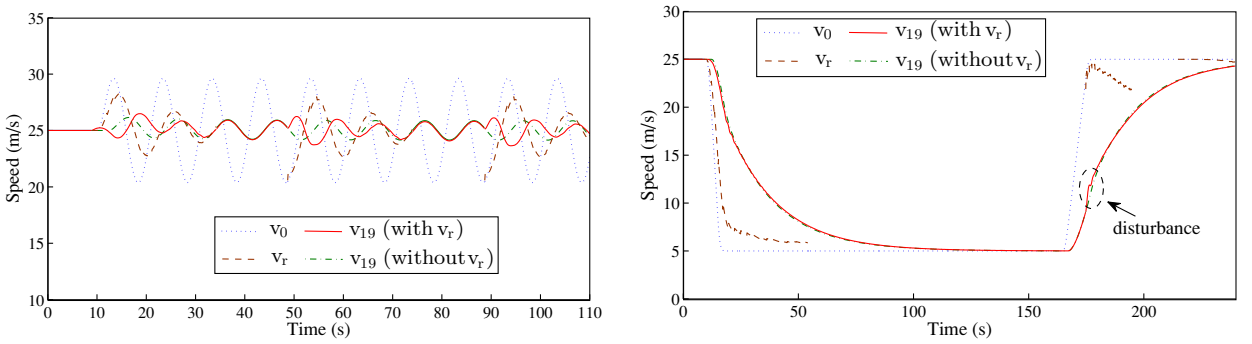

(a) Continuous small traffic perturbations (b) Single large perturbation

Fig. 10. Traffic flow **I** with local and front information in different perturbations scenarios.

whilst the initially independent clusters finally can merge into the big one when experiencing a single large perturbation (see Fig. 9(a)). This phenomenon essentially reflects the instability of the traffic flow.

5.3. Improved traffic control with both local and downstream information

In this section, we further evaluate the system performance by the improved consensus control algorithms Eq. (23) with the help of combined V2V and V2I communication (i.e. V2X), wherein the studied traffic flow is specified similarly to that in Section 5.2. We first assume the ideal V2I communication with no measurement error for the targeted sensing area and AP's coverage is 1000m with $C_r = 1$. In addition, we only consider vehicles to drive in the traffic perturbation scenario.

The speed profiles of vehicle 19 in the traffic flow **I** are given in Fig. 10. We can see that the traffic control algorithm of Eq. (23) with both local and downstream information exhibits a similar performance to Eq. (23) with the local information,

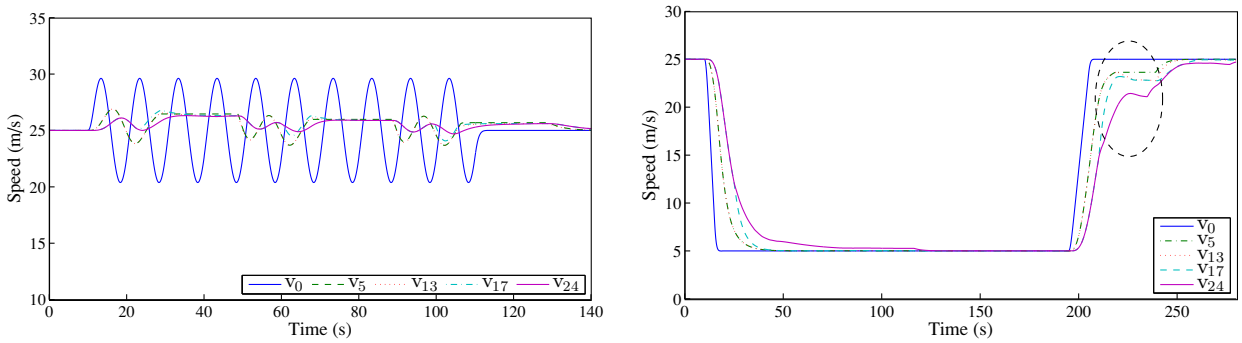

(a) Continuous small traffic perturbations (b) Single large perturbation

Fig. 11. Traffic flow **II** with local and front information in different perturbations scenarios.

which means, for the traffic flow **I** with the full communication connectivity, the downstream information cannot further improve the system performance in terms of perturbation mitigation. This is because the downstream traffic status can be quickly obtained by the following vehicles under the high-frequency beacon dissemination. In addition, due to the limited sensing coverage (300 m), the downstream reference speed v_r is unavailable in some cases, which may introduce an additional traffic disturbance when switching the driving strategy between the basic and improved consensus algorithms, as shown in Fig. 10(a).

For the traffic flow **II** under the regulation of our improved consensus algorithm, we can observe that the leading vehicles in different clusters started to decelerate/accelerate synchronously in both perturbation scenarios, as shown in Fig. 11. In addition, compared to the small perturbation in Fig. 11(a), the large perturbation (emergency event) in Fig. 11(b) is more sensitive to the upstream vehicles. The simulation results essentially indicate the improvement of traffic flow stability by using the downstream traffic information especially in the single large perturbation scenario as compared to that in Fig. 9(b) using only local information. However, the similar speed disturbance can be introduced (see Fig. 11(b)) due to the driving strategy switching caused by the inaccessible downstream information at some time or another. To mitigate such negative disturbance, an appropriate driving strategy switching should be further considered. This issue will be left in our future work.

5.4. Impact of V2I uncertainties and deployment

In this section, we evaluate the impacts of V2I uncertainties and deployment on the system performance. Specifically, we focus on the possibly introduced measurement errors from the roadside sensors and the deployment of V2I communication. The impact of packet loss and time delay in V2V communication has been studied in our previous work (Jia and Ngoduy, 2015) and is ignored here.

First, we consider the imperfect measurement of velocities in the targeted area, and evaluate its impact on the system performance. Normally, the measurement errors are assumed to follow some typical distribution models in the literature, such as normal distribution and uniform distribution (Patriota and Bolfarine, 2010). In this paper, we adopt a uniform distribution noise with zero mean for the speed measurement in the range of $[-\rho_v, \rho_v]$, $\rho_v > 0$, then explore the system performance in continuous small perturbations. It shall be noted that in case of adopting other model, e.g., standard derivation of a zero mean Gaussian noise, in the simulation, we can obtain similar results. Fig. 12(a) displays the speed profiles of leading vehicles in different clusters. We can observe that in the existence of the measurement error, the speed perturbations are still attenuated to the upstream traffic flow, which verified the efficiency of the proposed control algorithms on the perturbation mitigation. To investigate the impact of the measurement errors on the local traffic stability, the position errors of vehicle 29 to 28 within the same cluster under different ρ_v are shown in Fig. 12(b). It is observed that with the increasing measurement speed error, the position errors are enlarged accordingly. However, the position errors can be bounded by the measurement errors and maximum acceleration. It shall be noted that at $t = 50$ s, the position errors abruptly become large. This is because the received downstream reference speed has a sharp change when the neighbours of vehicle 29 pass by the AP, which leads to the large control errors. This issue can be improved by data process, e.g. noise filter, and will be left in our future work.

Second, we briefly evaluate the impact of V2I deployment on the system performance. Specifically, we consider two major factors: the AP's coverage and V2I beacon frequency. As illustrated in Fig. 1, the sensors are assumed to be fully deployed along the road and $C_r = 1$, which means the upstream vehicles can obtain the average speeds of the road segment between two downstream adjacent APs. We then consider the scenario that the leading vehicle 0 starts decelerate from 25 m/s to 5 m/s when passing by an AP. Fig. 13(b) shows the deceleration phase of the leading vehicle 24 in the fifth cluster under the different AP's coverages. It is observed that with the increasing AP's coverage, the speed of vehicle 24 has a quick reaction to the traffic perturbation, which indicates the improvement of the traffic flow stability. Similarly, the

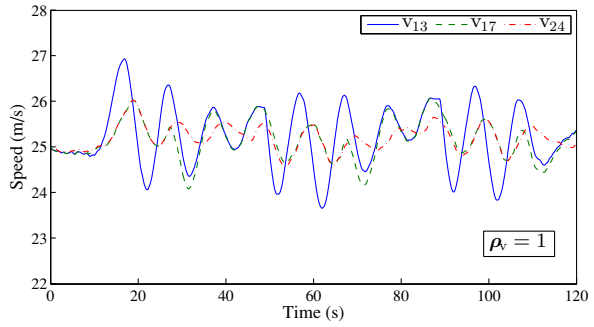

(a) Speed of leading vehicles in different clusters under continuous small perturbations

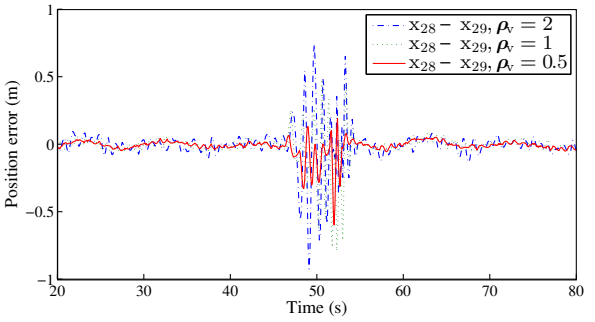

(b) Position error in a continuous small perturbations

Fig. 12. Impact of measurement errors on the system performance for traffic flow **II**.

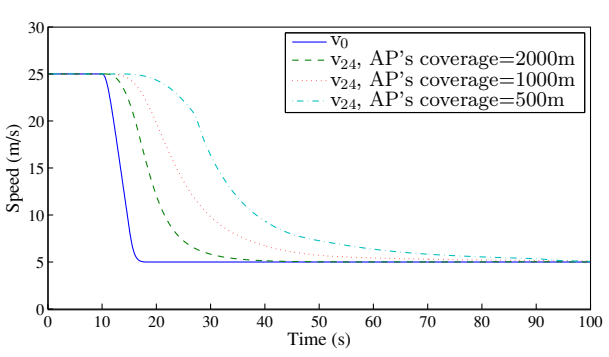

(a) Impact of AP's coverage

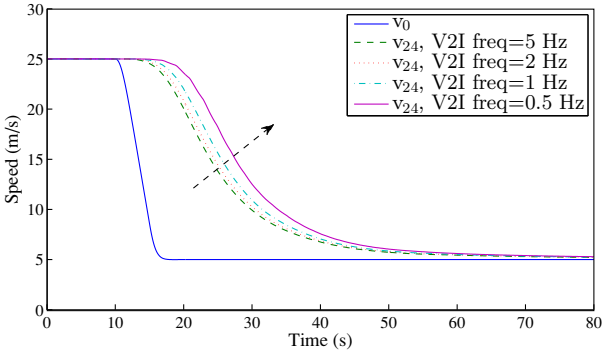

(b) Impact of V2I beacon frequency

Fig. 13. Impact of V2I deployment for traffic flow **II** in the single large perturbation.

increasing beacon frequency facilitates the following vehicle to quickly respond to the perturbation, as shown in Fig. 13(b). However, this improvement is no more significant when the beacon frequency reaches to a certain value, e.g., 2 Hz.

5.5. Further discussions

To summarise, the proposed local consensus-based CDS can guarantee the local stability and mitigate traffic perturbation for the fully connected traffic flow, however, it cannot maintain a better global stability for the partially connected traffic flow. Whilst the improved consensus-based CDS can further improve the traffic flow stability especially in case of a large perturbation. Moreover, the performance can be affected by many factors involved in the system. However, there are a few points which still cannot be addressed yet in this paper.

First, due to the unavailable downstream information in some cases (e.g., $C_r < 1$), the vehicle needs to switch the driving strategy between the basic control algorithm with local information and the improved control algorithm with both local and downstream information, which can introduce an additional perturbation, as shown in Figs. 10(a) and 11(b). To mitigate such negative impacts, the appropriate $\theta(t)$ in the envisioned traffic control Eq. (5) should be further investigated.

Second, due to the introduced measurement errors and the sharp change of the traffic status, the direct adoption of the collected downstream traffic status in the proposed control algorithms may impair the system performance, as shown in Fig. 12. This issue can be improved by data processing on the raw traffic information, e.g. Kalman filter, and will be left in our future work.

Third, the system analysis is based on a *second-order vehicle dynamics* described by Eqs. (2) and (3). In the presence of system uncertainties and physical limitations, including *actuator lags* and *sensing delays*, the vehicle dynamics will be modelled by a *third-order system* as below:

$$\dot{p}_i(t) = v_i(t) \tag{31}$$

$$\dot{v}_i(t) = a_i(t) \tag{32}$$

$$\dot{a}_i(t) = -\frac{1}{\omega_i}[a_i(t) - u_i(t-\varphi_i)] \tag{33}$$

where ω_i is the actuator lag, and φ_i is the sensing delay. In this system, the envisioned control algorithm with the help of acceleration information may further improve the robust performance of the CDS (Jin and Orosz, 2014). The theoretical analysis for such a third-order system is very cumbersome and will be left in our future work. Nevertheless, we have considered the factor of actuator lag in modelling vehicle dynamics in our simulations.

6. Concluding remarks

Recently, cooperative driving with the help of vehicular communications has attracted more concerns because it can significantly improve transportation efficiency and traffic safety. However, there still exist many issues unclear in terms of the system implementation. For example, how to design a suitable control algorithm according to the obtained traffic information via vehicular communications, how the deployment of infrastructure has impact on the system performance, etc.

To contribute to the state-of-the-art in traffic flow modelling and communications, we developed an enhanced cooperative driving system with the help of V2X communication, and proposed an improved consensus-based algorithm which takes into account both the local traffic information and the downstream traffic information. IEEE 802.11p, the defacto vehicular networking standard, was selected as the practical IVC protocols, and the roadside sensors were deployed to collect the average speed in the targeted area as the downstream traffic reference. We then theoretically analyzed how the system performance is affected by various possible uncertainties, such as communication delay and measurement errors. Numerical simulations have been conducted to evaluate our analysis in various traffic scenarios with different vehicular networking settings. Both the analysis and simulation results showed that under the proposed cooperative driving strategy, not only the local traffic flow stability is guaranteed, but also the shock waves are significantly smoothed.

Acknowledgements

This research was financially supported by the UK Engineering and Physical Sciences Research Council (EPSRC) Career Acceleration fellowship Grant EP/J002186/1.

Appendix A. Proof of Lemma 1

Proof. First, the following Lemma in literature is used for our proof:

Lemma 3 (proposed by Parks and Hahn (1992)). *Given a complex-coefficient polynomial*

$$p(s) = s^2 + (a+ib)s + c + id \tag{A.1}$$

where $a, b, c, d \in \mathbb{R}$, $p(s)$ *is stable if and only if* $a > 0$ *and* $abd + a^2c - d^2 > 0$.

Let λ be the eigenvalue of $\widetilde{F}_{n-1}$, then

$$\begin{aligned} det(\lambda I_{2n-2} - \widetilde{F}_{n-1}) &= \begin{vmatrix} \lambda I_{n-1} & -I_{n-1} \\ \gamma_1 \widetilde{L} & \lambda I_{n-1} + \gamma_2 \widetilde{L} \end{vmatrix} \\ &= det(\lambda^2 I_{n-1} + \gamma_2 \widetilde{L}\lambda I_{n-1} + \gamma_1 \widetilde{L}) \\ &= \prod_{i=1}^{n-1} (\lambda^2 + \gamma_2 \theta_i \lambda + \gamma_1 \theta_i) \end{aligned}$$

where $\theta_i \in \sigma(\widetilde{L})$. Thus the Hurwitz stability of matrix F is equivalent to that of polynomial: $R(\lambda) = \lambda^2 + \gamma_2\theta_i\lambda + \gamma_1\theta_i$, for all $\theta_i \in \sigma(\widetilde{L})$. Based on Lemma 3, we have:

(1) $Re(\theta_i) > 0$, which holds by the positive stable matrix $\widetilde{L}$.

(2) $\gamma_2^2\gamma_1 Re(\theta_i)(Im(\theta_i))^2 + \gamma_2^2\gamma_1(Re(\theta_i))^3 - \gamma_1^2(Im(\theta_i))^2 > 0$, which can be satisfied by the condition Eq. (16).

Thus the Lemma 1 holds. □

Appendix B. Proof of Theorem 1

Proof. We first consider Eq. (15b).

Based on Lemma 1, $\widetilde{F}_{n-1}$ is Hurwitz stable. Therefore, there exists a positive definite matrix $P \in \mathbb{R}^{(2n-2)\times(2n-2)}$ such that

$$P\widetilde{F}_{n-1} + \widetilde{F}_{n-1}^T P = -I_{2n-2} \tag{B.1}$$

Consider Lyapunov–Razumikhin candidate function $V(\widetilde{\chi}_{n-1}) = \widetilde{\chi}_{n-1}^T P \widetilde{\chi}_{n-1}$ and combine Eq. (15b), we have

$$\begin{aligned}\dot{V}(\widetilde{\chi}_{n-1}) &= \dot{\widetilde{\chi}}_{n-1}^T P \widetilde{\chi}_{n-1} + \widetilde{\chi}_{n-1}^T P \dot{\widetilde{\chi}}_{n-1} = \widetilde{\chi}_{n-1}^T (P\widetilde{F}_{n-1} + \widetilde{F}_{n-1}^T P)\widetilde{\chi}_{n-1} \\ &\quad - 2\int_{-\tau}^{0} \widetilde{\chi}_{n-1}^T P \widetilde{\mathcal{B}}_1 \widetilde{\mathcal{A}}_1 \widetilde{\chi}_{n-1}(t+s)ds - 2\int_{-\tau}^{0} \widetilde{\chi}_{n-1}^T P \widetilde{\mathcal{B}}_1^2 \widetilde{\chi}_{n-1}(t+s-\tau)ds\end{aligned}$$

It is well known that for any $a, b \in \mathbb{R}^n$ and any positive-definite matrix $\Omega \in \mathbb{R}^{n\times n}$, $2a^T b \le a^T \Omega^{-1} a + b^T \Omega b$. Thus

$$\begin{aligned}\dot{V}(\widetilde{\chi}_{n-1}) &\le \widetilde{\chi}_{n-1}^T (P\widetilde{F}_{n-1} + \widetilde{F}_{n-1}^T P)\widetilde{\chi}_{n-1} + \tau\, \widetilde{\chi}_{n-1}^T P \widetilde{\mathcal{B}}_1 \widetilde{\mathcal{A}}_0 P^{-1} \widetilde{\mathcal{A}}_0^T \widetilde{\mathcal{B}}_1^T P \widetilde{\chi}_{n-1} \\ &\quad + \int_{-\tau}^{0} \widetilde{\chi}_{n-1}^T (t+s) P \widetilde{\chi}_{n-1}(t+s)ds + \tau\, \widetilde{\chi}_{n-1}^T P \widetilde{\mathcal{B}}_1^2 P^{-1} \widetilde{\mathcal{B}}_1^{2T} P \widetilde{\chi}_{n-1} \\ &\quad + \int_{-\tau}^{0} \widetilde{\chi}_{n-1}^T (t+s-\tau) P \widetilde{\chi}_{n-1}(t+s-\tau)ds\end{aligned}$$

Choose $\phi_s = \zeta s$ where constant $\zeta > 1$. According to Lemma 2, in case of

$$V(\widetilde{\chi}_{n-1}(t-\theta)) \le \zeta V(\widetilde{\chi}_{n-1}(t)), 0 \le \theta \le 2\tau$$

we have

$$\dot{V}(\widetilde{\chi}_{n-1}) \le -\widetilde{\chi}_{n-1}^T \widetilde{\chi}_{n-1} + \tau\, \widetilde{\chi}_{n-1}^T (P\widetilde{\mathcal{B}}_1 \widetilde{\mathcal{A}}_0 P^{-1} \widetilde{\mathcal{A}}_0^T \widetilde{\mathcal{B}}_1^T P + P\widetilde{\mathcal{B}}_1^2 P^{-1} \widetilde{\mathcal{B}}_1^{2T} P + 2\zeta P)\widetilde{\chi}_{n-1}$$

Therefore, if we choose a suitable value of τ to render $\dot{V}(\widetilde{\chi}_{n-1}) < -\eta \widetilde{\chi}_{n-1}^T \widetilde{\chi}_{n-1}$ for some $\eta > 0$, by Lemma 2, we conclude

$$\lim_{t\to\infty} \widetilde{x}_{n-1}(t) = 0, \quad \text{and} \quad \lim_{t\to\infty} \widetilde{v}_{n-1}(t) = 0 \tag{B.2}$$

On the other hand, for Eq. (15a), note that $W^T \mathbf{1} = (\sqrt{n}, 0, \ldots, 0)^T$, we then have

$$x(t) - \frac{1}{\sqrt{n}}\widetilde{x}_0(t)\mathbf{1} = W(\widetilde{x}(t) - \frac{1}{\sqrt{n}}\widetilde{x}_0(t) W^T \mathbf{1}) = W(0^T, \widetilde{x}_{n-1}^T(t))^T$$

and

$$v(t) - \frac{1}{\sqrt{n}}\widetilde{v}_0(t)\mathbf{1} = W(\widetilde{v}(t) - \frac{1}{\sqrt{n}}\widetilde{v}_0(t) W^T \mathbf{1}) = W(0^T, \widetilde{v}_{n-1}^T(t))^T$$

According to Eq. (B.2), the above two equations approach 0 as $t \to \infty$, which imply Eq. (4) holds.

This completes the proof. □

Appendix C. Proof of Theorem 2

Proof. We first consider Eq. (27b).

Consider Lyapunov–Razumikhin candidate function $V(\bar{\chi}_k) = \bar{\chi}_k^T P \bar{\chi}_k$, where

$$P = \begin{bmatrix} \beta_2 I_{n-1} & \beta_1 I_{n-1} \\ \beta_1 I_{n-1} & \beta_2 I_{n-1} \end{bmatrix}, \quad \beta_2 > \beta_1 > 0$$

is positive definite. then

$$\begin{aligned}\dot{V}(\widetilde{\chi}_{n-1}) &= \dot{\widetilde{\chi}}_{n-1}^T P \widetilde{\chi}_{n-1} + \widetilde{\chi}_{n-1}^T P \dot{\widetilde{\chi}}_{n-1} = \widetilde{\chi}_{n-1}^T (P\widetilde{F}_{n-1} + \widetilde{F}_{n-1}^T P)\widetilde{\chi}_{n-1} - 2\int_{-\tau}^{0} \widetilde{\chi}_{n-1}^T P \widetilde{\mathcal{B}}_1 \widetilde{\mathcal{A}}_1 \widetilde{\chi}_{n-1}(t+s)ds \\ &\quad - 2\int_{-\tau}^{0} \widetilde{\chi}_{n-1}^T P \widetilde{\mathcal{B}}_1^2 \widetilde{\chi}_{n-1}(t+s-\tau)ds - 2\int_{-\tau}^{0} \widetilde{\chi}_{n-1}^T P \widetilde{\mathcal{B}}_1 \widetilde{\Delta}_{n-1}(t+s)ds + 2\widetilde{\chi}_{n-1}^T P \widetilde{\Delta}_{n-1}\end{aligned}$$

We adopt the similar method of Theorem 2 in (Jia and Ngoduy, 2015), then we can verify if parameters β_1 and β_2 satisfy Eq. (28), the $\widetilde{\chi}_{n-1}$ is uniformly ultimately bounded by C_0.

On the other hand, for Eq. (27a), we have

$$\begin{aligned}\left\|\bar{x}(t) - \frac{1}{\sqrt{n}}\widetilde{x}_0(t)\mathbf{1}\right\| &= \left\|W(\widetilde{x}(t) - \frac{1}{\sqrt{n}}\widetilde{x}_0(t) W^T \mathbf{1})\right\| = \left\|W\left(\left(\int_0^t \int_0^s \delta_0(r)drds\right)^T, \widetilde{x}_{n-1}^T(t)\right)^T\right\| \\ &\le \|W\| \max\{\mu Q_2, C_0\}\end{aligned}$$

and

$$\left\|\tilde{v}(t)-\frac{1}{\sqrt{n}}\tilde{v}_0(t)\mathbf{1}\right\| = \left\|W(\tilde{v}(t)-\frac{1}{\sqrt{n}}\tilde{v}_0(t)W^T\mathbf{1})\right\| = \left\|W\left(\left(\int_0^t \delta_0(s)ds\right)^T, \tilde{v}_{n-1}^T(t)\right)^T\right\|$$
$$\leq \|W\|\max\{\mu\varrho_1, C_0\}$$

where $\mu=\beta_1\sum_{j=1}^{n}a_{ij}(j-i)T+\beta_2$ according to the Eq. (22). Thus the above two equations are uniformly ultimately bounded, which imply Eq. (29) holds. □

References

van Arem, B., van Driel, C.J.G., Visser, R., 2006. The impact of cooperative adaptive cruise control on traffic-flow characteristics. IEEE Transactions on Intelligent Transportation Systems 7 (4), 429–436.

Bernardo, M., Salvi, A., Santini, S., 2015. Distributed consensus strategy for platooning of vehicles in the presence of time-varying heterogeneous communication delays. IEEE Transactions on Intelligent Transportation Systems 16 (1), 102–112.

Fernandes, P., 2012. Platooning with ivc-enabled autonomous vehicles: strategies to mitigate communication delays, improve safety and traffic flow. IEEE Transactions on Intelligent Transportation Systems 13, 91–106.

Forster, M., Frank, R., Gerla, M., Engel, T., 2014. A cooperative advanced driver assistance system to mitigate vehicular traffic shock waves. In: Proceedings of IEEE INFOCOM, pp. 1968–1976.

Ghasemi, A., Kazemi, R., Azadi, S., 2013. Stable decentralized control of a platoon of vehicles with heterogeneous information feedback. IEEE Transactions on Vehicular Technology 62 (9), 4299–4308.

Hale, J.K., Lunel, S.M.V., 1993. Introduction to Functional Differential Equations. Springer-Verlag.

Hao, H., Barooah, P., 2012. Stability and robustness of large vehicular platoons with linear and nonlinear decentralized control for two architectures. International Journal of Robust and Nonlinear Control 23 (18), 2097–2122.

Jia, D., Lu, K., Wang, J., 2014. A disturbance-adaptive design for vanet-enabled vehicle platoon. IEEE Transactions on Vehicular Technology 63 (2), 527–539.

Jia, D., Lu, K., Wang, J., Zhang, X., Shen, X., 2016. A survey on platoon-based vehicular cyber-physical systems. IEEE Communications Surveys and Tutorials 18 (1), 263–284.

Jia, D., Ngoduy, D., 2016. Platoon based cooperative driving model with consideration of realistic inter-vehicle communication. Transportation Research Part C 68, 245–264.

Jin, I.G., Orosz, G., 2014. Dynamics of connected vehicle systems with delayed acceleration feedback. Transportation Research Part C 46 (9), 46–64.

Jin, W.L., Recker, W.W., 2006. Instantaneous information propagation in a traffic stream through inter-vehicle communication. Transportation Research Part B 40, 230–250.

Jin, W.L., Wang, H.J., 2008. Modeling connectivity of inter-vehicle communication systems with road-side stations. The Open Transportation Journal 2, 1–6.

Kesting, A., Treiber, M., Helbing, D., 2010a. Enhanced intelligent driver model to access the impact of driving strategies on traffic capacity. Philosophical Transactions of the Royal Society A 368, 4585–4605.

Kesting, A., Treiber, M., Helbing, D., 2010b. Connectivity statistics of store-and-forward inter-vehicle communication. IEEE Transactions on Intelligent Transportation Systems 11, 172–181.

Kesting, A., Treiber, M., Schonhof, M., Helbing, D., 2008. Adaptive cruise control design for active congestion avoidance. Transportation Research Part C 16 (6), 668–683.

Laval, J.A., Leclercq, L., 2008. Microscopic modeling of the relaxation phenomenon using a macroscopic lane-changing model. Transportation Research Part B 42, 511–522.

Laval, J.A., Toth, C.S., Zhou, Y., 2014. A parsimonious model for the formation of oscillations in car-following models. Transportation Research Part B 70, 228–238.

Ma, X., Martensson, J., 2012. Optimal controls of vehicle trajectories in fleet management using v2i information. In: Proceedings of International Conference on Connected Vehicles and Expo (ICCVE), pp. 256–261.

Middleton, R., Braslavsky, J., 2012. String instability in classes of linear time invariant formation control with limited communication range. IEEE Transactions on Automatic Control 55 (7), 1519–1530.

Milanes, V., Villagra, J., Godoy, J., Simo, J., Perez, J., Onieva, E., 2012. An intelligent v2i-based traffic management system. IEEE Transactions on Intelligent Transportation Systems 13 (1), 49–58.

Naus, G.J.L., Vugts, R.P.A., Wang, J., Ploeg, J., van de Molengraft, M.R.J.G., Steinbuch, M., 2010. String-stable cacc design and experimental validation: A frequency-domain approach. IEEE Transactions on Vehicular Technology 59 (9), 4268–4279.

Ngoduy, D., 2013a. Analytical studies on the instabilities of heterogeneous intelligent traffic flow. Communications in Nonlinear Science and Numerical Simulation 18 (10), 2699–2706.

Ngoduy, D., 2013b. Platoon-based macroscopic model for intelligent traffic flow. Transportmetrica B 1 (2), 153–169.

Ngoduy, D., 2015. Effect of the car-following combinations on the instability of heterogeneous traffic flow. Transportmetrica B 3 (1), 44–58.

Ngoduy, D., Jia, D., 2016. Multi anticipative bidirectional macroscopic traffic model considering cooperative driving strategy. Transportmetrica B doi:10.1080/21680566.2016.1142401. (in press)

Ngoduy, D., Wilson, R.E., 2014. Multi-anticipative nonlocal macroscopic traffic model. Computer-Aided Civil and Infrastructure Engineering 29, 248–263.

Olfati-Saber, R., Fax, J.A., Murray, R., 2007. Consensus and cooperation in networked multi-agent systems. In: Proceedings of the IEEE. vol. 95 (1), pp. 1968–1976.

Oncu, S., van de Wouw, N., Nijmeijer, H., 2011. Cooperative adaptive cruise control: tradeoffs between control and network specifications. The 14th International IEEE Conference on Intelligent Transportation Systems (ITSC). Washington, DC, pp. 2051–2056.

Parks, P.C., Hahn, V., 1992. Stability Theory. Prentice-Hall, Upper Saddle River, NJ.

Patriota, A.G., Bolfarine, H., 2010. Measurement error models with a general class of error distribution. Statistics 44 (2), 119–127.

Ploeg, J., Semsar-Kazerooni, E., Lijster, G., van de Wouw, N., Nijmeijer, H., 2013. Graceful degradation of cacc performance subject to unreliable wireless communication. The 16th International IEEE Conference on Intelligent Transportation Systems (ITSC). The Hague, pp. 1210–1216.

Ren, W., 2007. Information consensus in multivehicle cooperative control. IEEE Control Systems Magazine 27 (2), 71–82.

Ren, W., Beard, R.W., 2005. Consensus seeking in multiagent systems under dynamically changing interaction topologies. IEEE Transactions on Automatic Control 50 (5), 655–661.

Saifuzzaman, M., Zheng, Z., 2014. Incorporating human-factors in car-following models: a review of recent developments and research needs. Transportation Research Part C 48, 379–403.

Saifuzzaman, M., Zheng, Z., Haque, M.M., Washington, S., 2015. Revisiting the taskcapability interface model for incorporating human factors into car-following models. Transportation Research Part B 82, 1–19.

Segata, M., Joerer, S., Bloessl, B., Sommer, C., Dressler, F., Cigno, R.L., 2014. Plexe: a platooning extension for veins. In: Proceedings of the 6th IEEE Vehicular Networking Conference, Paderborn, Germany, pp. 53–60.

Treiber, M., Kesting, A., Helbing, D., 2006. Delays, inaccuracies and anticipation in microscopic traffic model. Physica A 360, 71–88.

Wang, L.Y., Syed, A., Yin, G., Pandya, A., Zhang, H., 2012. Coordinated vehicle platoon control: weighted and constrained consensus and communication network topologies. In: Proceedings of the 51st IEEE Conference on Decision and Control, pp. 4057–4062.
Wang, M., Daamen, W., Hoogendoorn, S.P., van Arem, B., 2014. Rolling horizon control framework for driver assistance systems. part ii: cooperative sensing and cooperative control. Transportation Research Part C 40 (3), 290–311.
Wang, M., Treiber, M., Daamen, W., Hoogendoorn, S.P., van Arem, B., 2013. Modelling supported driving as an optimal control cycle: framework and model characteristics. Transportation Research Part C 80 (7), 491–511.
Wang, X., 2007. Modeling the process of information relay through inter-vehicle communications. Transportation Research Part B 41, 684–700.
Wang, X., Adams, T.M., Jin, W.L., Meng, Q., 2010. The process of information propagation in a traffic stream with a general vehicle headway: a revisit. Transportation Research Part C 18 (3), 367–375.
Zheng, Z., 2014. Recent developments and research needs in modeling lane changing. Transportation Research Part B 60, 16–32.
Zheng, Z., Ahn, S., Chen, D., Laval, J.A., 2013. The effects of lane-changing on the immediate follower: anticipation, relaxation, and change in driver characteristics. Transportation Research Part C 26, 367–379.